한국복합신소재구조학회 논문집 제4권, 제4호, 2013년 12월
J. Korean Soc. Adv. Comp. Struc. Vol. 4, No. 4, pp. 1-8, December 2013
DOI http://dx.doi.org/10.11004/kosacs.2013.4.4.001

ISSN 2093-5145(Print)
ISSN 2288-0232(Online)

편심재하된 하이브리드 FRP-콘크리트 합성 기둥의 구조적 특성

최진우[1] · 서수홍[2] · 박준석[3] · 주형중[4] · 윤순종[5]

홍익대학교 토목공학과 박사과정[1], ㈜아이시스이엔씨 팀장[2],
서일대학교 토목과 조교수[3], ㈜아이시스이엔씨 대표이사[4], 홍익대학교 토목공학과 교수[5]

The Structrual Behavior of Eccentrically Loaded Hybrid FRP-Concrete Composite Columns

Choi, Jin-Woo[1] · Seo, Su-Hong[2] · Park, Joon-Soek[3] · Joo, Hyung-Joong[4] · Yoon, Soon-Jong[5]

[1]PhD. Candidate, Department of Civil Engineering, Hongik University, Seoul, Korea
[2]Team Manager, ISIS E&C, Seoul, Korea
[3]Assistant Professor, Department of Civil Engineering, Seoil University, Seoul, Korea
[4]President, ISIS E&C, Seoul, Korea
[5]Professor, Department of Civil Engineering, Hongik University, Seoul, Korea

Abstract: Pile foundations constructed by the fiber reinforced polymer plastic piles have been used in coastal and oceanic regions in many countries. Generally, fiber reinforced polymer plastic piles are consisted of filament winding FRP which is used to wrap the outside of concrete pile to increase the axial load carrying capacity or pultruded FRP which is located in the core concrete to resist the bending moment arising due to eccentric loading. In this paper, the analytical procedures of hybrid concrete filled FRP tube flexural members are suggested based on the CFT design method. Moreover, the analytical results are compared with the experimental results to obtained by the previous researches. The results of comparison analyses are performed to estimate the accuracy of the analytical procedure for hybrid FRP-concrete composite compression test, members under eccentrical loading.

Key Words: Hybrid concrete filled FRP tube member, plastic stress distribution method, strain compatibility method, flexural test

1. INTRODUCTION

Existing steel and/or concrete piles are widely applied in civil engineering industries with long time experience and they have many advantages. However, steel pipe pile or concrete filled steel tube (CFT) pile, which is the most common steel piles, are prone to losing their structural integrity over time due to corrosive and humid environmental conditions. Moreover, concrete piles such as in-situ concrete piles and pretensioned spun high strength concrete (PHC) piles are subject to deterioration of their long-term structural durability. Permeability of the exposed concrete by water can cause the concrete to deteriorate over time. Furthermore, corrosion is known to occur in the reinforcing steel rebars used inside concrete piles (Joo, 2010).

In the previous researches (Choi et al., 2010; Shin, 2010; Choi et al., 2011a; Choi et al., 2011b; An, 2011; Choi et al. 2012; Kang, 2012), hybrid concrete filled FRP tube (HCFFT) pile was developed. The characteristics of structural behavior under compression and/or flexure for HCFFT piles was investigated through the experimental and analytical studies. HCFFT pile is consisted of pultruded FRP

주요어: 하이브리드 FRP-콘크리트 합성 부재, 소성응력분배법, 변형률적합법, 휨실험

Corresponding author: Yoon, Soon-Jong
Department of Civil Engineering, Hongik University, 72-1 Sangsu-dong, Mapo-gu, Seoul 172-732, Korea.
Tel: +82-2-3141-0774, Fax: +82-2-3141-0774, E-mail: sjyoon@hongik.ac.kr

투고일: 2013년 11월 4일 / 수정일: 2013년 11월 27일 / 게재확정일: 2013년 12월 11일

(PFRP) unit module, filament winding FRP (FFRP) which is in the outside of mandrel composed of circular shaped assembly of PFRP unit modules, and core concrete which is casted inside of the circular tube shaped hybrid FRP pile (Lee, et al., 2011; Choi, et al., 2012) as shown in Fig. 1.

In this paper, the flexural analysis procedures of hybrid FRP-concrete composite piles are suggested based on the CFT pile design method. Moreover, the analytical results are compared with the experimental results obtained in the previous researches (Choi et al., 2012; Kang, 2012). The results of comparison analyses are used to estimate the accuracy of analysis procedure for hybrid FRP-concrete composite flexural members.

Fig. 1 HCFFT Piles (Kang, 2012)

2. FLEXURAL ANALYSIS OF HCFFT MEMBERS

The flexural analysis procedures of HCFFT members are suggested by referring to the analysis procedure for CFT members. The evaluation of flexural strength for the CFT members is incorporated in the several codes such as Specification for Structural Steel Buildings (American Institute of Steel Construction, 2005), ACI Building Code (American Concrete Institute, 2008a), etc. (Kim, 2010; Beheshti-Aval, 2012). The flexural strength for the CFT members can be obtained either by using the plastic stress distribution method as given in AISC specification (2005) or by the strain compatibility method as given in ACI code (2008a). In this paper, two analysis methods, i.e., the plastic stress distribution method and the strain compatibility method, for the HCFFT members are discussed.

In the previous research (Fam et al., 2002), the experimental studies were conducted to estimate the confinement effect for the compression zone of concrete filled FRP tube (CFFT) flexural members. From the experimental results, the relationship between axial strain and lateral strain is linear, with a slope proportional to the longitudinal Poisson's ratio of the tube, which indicates lack of confinement effect (American Concrete Institute, 2008b). Therefore, it is assumed that there is no confinement effect of the HCFFT members because of narrow compression zone of the member under flexure.

1. The Plastic Stress Distribution Method

In the plastic stress distribution method for CFT member, it is assumed that the whole cross-section of steel tube and concrete is approached to the plastic state at the failure as shown in Fig. 2 (Kim, 2010; Beheshti-Aval, 2012). Moreover, other assumptions for the plastic stress distribution analysis are given below (Kim, 2010).

(1) At the ultimate state, the stress distribution of steel is constant and whole cross-section of steel tube reached to its yield strength.

(2) At the ultimate state, the stress distribution of concrete is constant and ultimate strength is $0.85f_{ck}$ at the rectangular cross-section and $0.95f_{ck}$ at the circular cross-section.

(3) The tensile strength of concrete is neglected.

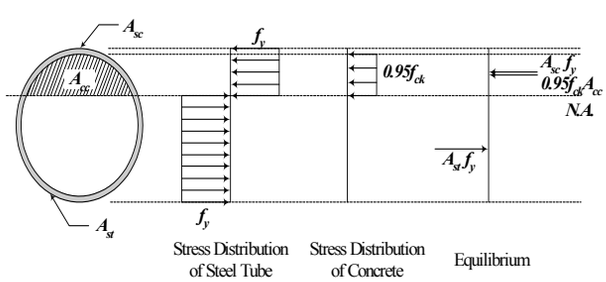

Fig. 2 The Stress Distribution in CFT Cross-section According to the Plastic Stress Distribution Method (Kim, 2010; Beheshti-Aval, 2012)

To derive the analysis procedure using the plastic stress distribution method for HCFFT members, the nomenclature and stress distribution in the cross-section of HCFFT member are shown in Fig. 3.

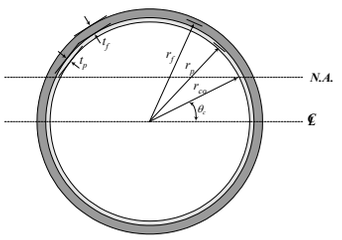

(a) Nomenclature

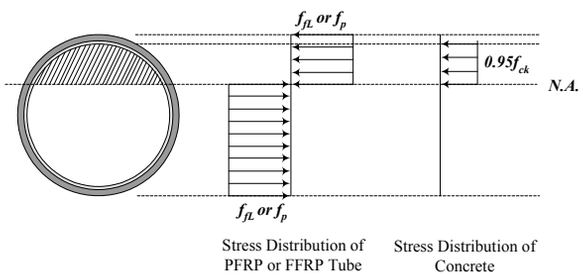

(b) Stress Distribution

Fig. 3 Derivation for HCFFT Flexural Member Using the Plastic Stress Distribution Method

The strength of PFRP and FFRP in the compression zone is derived as Eqs. (1) and (2), respectively. Moreover, the strength of PFRP and FFRP in the tension zone is derived as Eqs. (3) and (4), respectively.

$$P_{pc} = f_p t_p r_p (\pi - 2\theta_c) \tag{1}$$

$$P_{fc} = f_{fL} t_f r_f (\pi - 2\theta_c) \tag{2}$$

$$P_{pt} = f_p t_p r_p (\pi + 2\theta_c) \tag{3}$$

$$P_{ft} = f_{fL} t_f r_f (\pi + 2\theta_c) \tag{4}$$

In Eq. (1) to Eq. (4), P is the axial load carrying capacity and subscripts p, f, c, and t are the PFRP, FFRP, compression zone, and tension zone, respectively. Moreover, f_p, t_p, and r_p are the tensile strength, thickness, and radius of PFRP, f_{fL}, t_f, and r_f are the tensile strength, thickness, and radius of FFRP, and θ_c is the neutral angle, respectively.

The neutral angle is a function not only the axial load carrying capacity for PFRP and FFRP but also for concrete. Therefore, compressive strength of concrete is derived as Eq. (5).

$$P_c = \frac{0.95 f_{co} D_{co}^2 \left[\frac{\pi}{2} - \left(\theta_c + \frac{sin(2\theta_c)}{2} \right) \right]}{4} \tag{5}$$

In Eq. (5), P_c is the axial load carrying capacity and D_{co} is the diameter of concrete, respectively.

The flexural load carrying capacity of HCFFT members can be obtained by multiplying the results of Eq. (1) to Eq. (5) and the distance between neutral axis and the centroid of cross-section in the tension or compression zone, respectively. The flexural load carrying capacity of HCFFT members composed of PFRP and FFRP in the compression zone is expressed as Eq. (6) and in the tension zone is expressed as Eq. (7), respectively. Moreover, the flexural load carrying capacity of concrete in the compression zone is expressed as Eq. (8). The summation of results obtained from Eq. (6) to Eq. (8) is the flexural load carrying capacity of HCFFT expressed as Eq. (9).

$$\begin{aligned} M_{frpc} &= f_p t_p r_p (\pi - 2\theta_c) \left[\frac{2\left[\left(r_p + \frac{t_p}{2} \right)^3 - \left(r_p - \frac{t_p}{2} \right)^3 \right]}{3 t_p r_p (\pi - \theta_c)} - r_p + c \right] \\ &+ f_{fL} t_f r_f (\pi - 2\theta_c) \left[\frac{2\left[\left(r_f + \frac{t_f}{2} \right)^3 - \left(r_f - \frac{t_f}{2} \right)^3 \right]}{3 t_f r_f (\pi - \theta_c)} - r_f + c \right] \end{aligned} \tag{6}$$

$$\begin{aligned} M_{frpt} &= f_p t_p r_p (\pi + 2\theta_c) \left[\frac{2\left[\left(r_p + \frac{t_p}{2} \right)^3 - \left(r_p - \frac{t_p}{2} \right)^3 \right]}{3 t_p r_p (\pi - \theta_c)} - r_p + c \right] \\ &+ f_{fL} t_f r_f (\pi + 2\theta_c) \left[\frac{2\left[\left(r_f + \frac{t_f}{2} \right)^3 - \left(r_f - \frac{t_f}{2} \right)^3 \right]}{3 t_f r_f (\pi - \theta_c)} - r_f + c \right] \end{aligned} \tag{7}$$

$$M_c = \frac{0.95 f_{co} D_{co}^{\,2}\left[\frac{\pi}{2} - \left(\theta_c + \frac{sin(2\theta_c)}{2}\right)\right]}{4} \times \left[\frac{D_{co}}{3}\left(\frac{sin^{\,3}(\theta_c)}{\frac{\pi}{2} - \theta_c - sin\,(\theta_c)\cos(\theta_c)}\right)\right] \quad (8)$$

$$M_{HCFFT} = M_{frpc} + M_{frpt} + M_c \quad (9)$$

In Eq. (6) to Eq. (8), c is the distance from top extreme fiber to neutral axis as given in Eq. (10)

$$c = r_{co}(1 - sin(\theta_c)) \quad (10)$$

2. The Strain Compatibility Method

In the strain compatibility method for CFT member, it is assumed that the stress distribution of steel tube is linear until the material reached to its yield strength and constant after material yielding, as shown in Fig. 4. The strain compatibility method determines the flexural load carrying capacity when the extreme fiber at the tension zone reached to yield or fail. Moreover, other assumptions for the strain compatibility method are given below (Kim, 2010).

(1) The strain distribution in the cross-section is linear.

(2) The nominal moment is determined when the strain of concrete at the extreme fiber is 0.003.

(3) For the stress distribution of steel and concrete, the test data or qualified model can be used.

(4) The tensile strength of concrete is neglected.

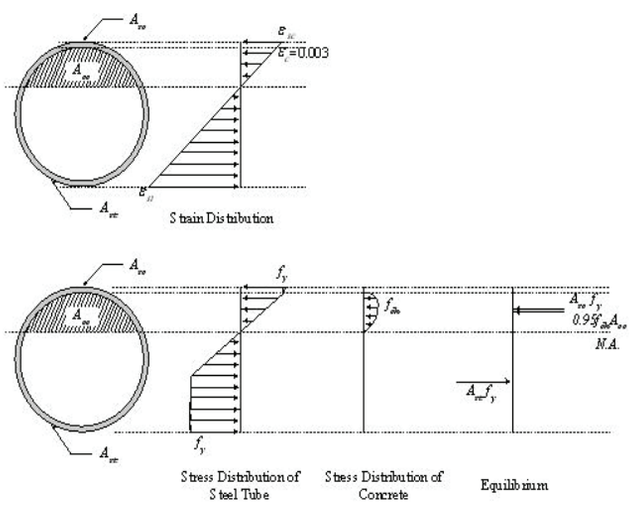

Fig. 4 Strain and Stress Distribution in CFT Cross-Section According to the Strain Compatibility Method (Kim, 2010; Beheshti-Aval., 2012)

In case of CFT member, the elastic modulus of steel is about 8 times larger than that of concrete, in general. However, the elastic modulus of FRP and concrete are nearly the same. Therefore, it can be assumed that the stress distribution of PFRP, FFRP, and concrete is nearly the same.

In addition, the neutral axis must be located above the center line of cross-section because the cross-section of HCFFT is symmetric and the relationship between stress and strain is almost linear. Therefore, PFRP and FFRP must be failed at the bottom extreme fiber (i.e., tension zone of the member).

The derivation procedure of the flexural strength for HCFFT member is shown in Fig. 5. In Fig 5, the areas of small elements for PFRP and FFRP are expressed as Eq. (11) and Eq. (12), respectively.

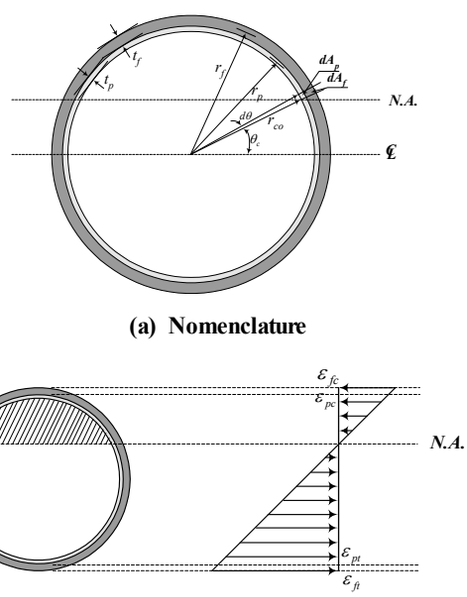

(a) Nomenclature

(b) Stress Distribution

Fig. 5 Derivation for HCFFT Flexural Member Using the Strain Compatibility Method

$$dA_p = 2t_p r_p d\theta \quad (11)$$

$$dA_f = 2t_f r_f d\theta \quad (12)$$

In Eq. (11) and Eq. (12), A_p and A_f are the area of PFRP and FFRP, respectively. Moreover, from the linear strain distribution of PFRP and FFRP as shown in Fig 5, the proportional expressions can be obtained as shown in Eq. (13) and Eq. (14).

$$\epsilon_{pt} : \epsilon_p = 2r_p - c : \left(r_p + \frac{t_p}{2}\right) sin(\theta) + \left(r_p + \frac{t_p}{2} - c\right) \tag{13}$$

$$\epsilon_{ft} : \epsilon_f = 2r_f - c : \left(r_f + \frac{t_f}{2}\right) sin(\theta) + \left(r_f + \frac{t_f}{2} - c\right) \tag{14}$$

In Eq. (13) and Eq. (14), ϵ_{pt} and ϵ_{ft} is the strain of PFRP and FFRP at the bottom extreme fiber and ϵ_p and ϵ_f is the strain distribution of PFRP and FFRP, respectively. To solve the Eq. (13) and Eq. (14), strain distribution equations are obtained as Eq. (15) and Eq. (16).

$$\epsilon_p = \frac{\left(r_p + \frac{t_p}{2}\right) sin(\theta) + \left(r_p - \frac{t_p}{2}\right) sin(\theta_c)}{2r_p - \left(r_p - \frac{t_p}{2}\right)(1 - \sin(\theta_c))} \epsilon_{pu} \tag{15}$$

$$\epsilon_f = \frac{\left(r_f + \frac{t_f}{2}\right) sin(\theta) + \left(r_f - \frac{t_f}{2}\right) sin(\theta_c)}{2r_f - \left(r_f - \frac{t_f}{2}\right)(1 - \sin(\theta_c))} \epsilon_{fu} \tag{16}$$

In Eq. (15) and Eq. (16), ϵ_{pu} and ϵ_{fu} is the ultimate strain of PFRP and FFRP, respectively. According to the Hooke's law, the stress distribution of PFRP and FFRP can be obtained by multiplying the results of Eq. (15) and/or Eq. (16) by the elastic modulus, and the strength of FRP in the compression and tension zone is obtained as Eqs. (17) and (18), respectively.

$$P_{frpc} = \int_{\theta_c}^{\frac{\pi}{2}} \left[\frac{2f_p r_p t_p \left[\left(r_p + \frac{t_p}{2}\right) |sin(\theta)| + \left(r_p - \frac{t_p}{2}\right) sin(\theta_c) \right]}{2r_p - \left(r_p - \frac{t_p}{2}\right)(1 - sin(\theta_c))} + \frac{2f_f r_f t_f \left[\left(r_f + \frac{t_f}{2}\right) |sin(\theta)| + \left(r_f - \frac{t_f}{2}\right) sin(\theta_c) \right]}{2r_f - \left(r_f - \frac{t_f}{2}\right)(1 - sin(\theta_c))} \right] d\theta \tag{17}$$

$$P_{frpt} = \int_{-\frac{\pi}{2}}^{\theta_c} \left[\frac{2f_p r_p t_p \left[\left(r_p + \frac{t_p}{2}\right) |sin(\theta)| + \left(r_p - \frac{t_p}{2}\right) sin(\theta_c) \right]}{2r_p - \left(r_p - \frac{t_p}{2}\right)(1 - sin(\theta_c))} + \frac{2f_f r_f t_f \left[\left(r_f + \frac{t_f}{2}\right) |sin(\theta)| + \left(r_f - \frac{t_f}{2}\right) sin(\theta_c) \right]}{2r_f - \left(r_f - \frac{t_f}{2}\right)(1 - sin(\theta_c))} \right] d\theta \tag{18}$$

In this paper, the stress distribution of concrete is regarded as the same as that in the plastic stress distribution method, as shown in Eq. (5). The Whitney's rectangular stress block model that is popular and qualified stress distribution model for concrete have been used in the civil engineering part for a long time. Therefore, in this paper, the Whitney's rectangular stress block model is used for the analysis of concrete flexural members.

Finally, the flexural load carrying capacity of HCFFT members can be obtained by multiplying the results of Eq. (17), Eq. (18), and Eq. (5) by the distance between neutral axis and the centroid of cross-section in the tension or compression zone, respectively. The flexural load carrying capacity of PFRP and FFRP in the compression zone is expressed as Eq. (19) and in the tension zone is expressed as Eq. (20), respectively. Moreover, the flexural load carrying capacity of concrete in the compression zone and HCFFT members can be used as Eq. (8) and Eq. (9).

The strain compatibility method must be solved the integral equation because it needs to consider the nonuniform stress distribution. Therefore, the analysis procedure using strain compatibility method is more complicated than that of the plastic stress distribution method.

$$M_{frpc} = \int_{\theta_c}^{\frac{\pi}{2}} \left[\frac{2f_p r_p^2 t_p \left[\left(r_p + \frac{t_p}{2}\right) |sin(\theta)| + \left(r_p - \frac{t_p}{2}\right) sin(\theta_c) \right]}{2r_p - \left(r_p - \frac{t_p}{2}\right)(1 - sin(\theta_c))} + \frac{2f_f r_f^2 t_f \left[\left(r_f + \frac{t_f}{2}\right) |sin(\theta)| + \left(r_f - \frac{t_f}{2}\right) sin(\theta_c) \right]}{2r_f - \left(r_f - \frac{t_f}{2}\right)(1 - sin(\theta_c))} \right] |sin(\theta)| d\theta \tag{19}$$

$$M_{frpt} = \int_{-\frac{\pi}{2}}^{\theta_c} \left[\frac{2f_p r_p^2 t_p \left[\left(r_p + \frac{t_p}{2}\right) |sin(\theta)| + \left(r_p - \frac{t_p}{2}\right) sin(\theta_c) \right]}{2r_p - \left(r_p - \frac{t_p}{2}\right)(1 - sin(\theta_c))} + \frac{2f_f r_f^2 t_f \left[\left(r_f + \frac{t_f}{2}\right) |sin(\theta)| + \left(r_f - \frac{t_f}{2}\right) sin(\theta_c) \right]}{2r_f - \left(r_f - \frac{t_f}{2}\right)(1 - sin(\theta_c))} \right] |sin(\theta)| d\theta \tag{20}$$

3. FLEXURAL TEST OF HCFFT

In the previous researches (Choi et al., 2012; Kang, 2012), the flexural test on the HCFFT specimens were conducted to estimate the flexural strength of HCFFT specimens. A total of 9 specimens, 3 sets of test with 3 specimens for each set, were tested under 4-point bending loads as shown in Fig. 6.

In the test, specimens with 3 different thicknesses of FFRPs, i.e., $2.8mm$, $4.2mm$, and $5.6mm$, are used. The descriptions on the specimens are given in Table 1 (Choi, et al., 2012; Kang, 2012). The mechanical properties of PFRP and FFRP used in the flexural test of HCFFT specimens are summarized in Table 2.

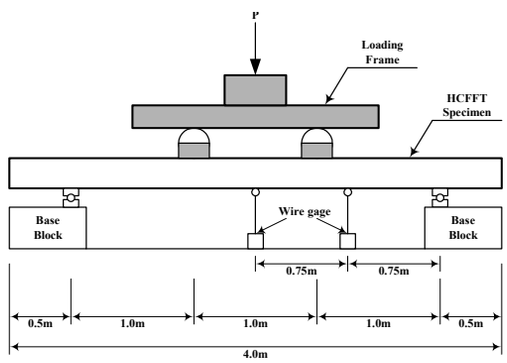

Fig. 6 Schematic View of 4-Point Bending Test Set-up (Choi et al., 2012; Kang, 2012)

Table 1. Description of HCFFT Specimens

Diameter (mm)	Length (m)	Specified Concrete Strength (MPa)	FFRP Thickness (mm)	No. of Specimen (EA)
300	4,000	23	2.8	3
			4.2	3
			5.6	3
Total				9

The wire gages were installed at the center and quarter point of specimens to measure deflections. Specimens are fixed at the supports by using a guide device because of the circular cross-section. All of the specimens were tested with a loading speed of 5 mm/mm and loads and displacements are measured and recorded automatically using computer controlled data acquisition system. The test set-up of flexural tests of HCFFT member is shown in Fig. 7 (Kang, 2012).

Table 2. Mechanical Properties of PFRP and FFRP (Choi et al, 2012)

Description		Thickness (mm)	Ultimate Strength (MPa)	Elastic Modulus (GPa)
FFRP	Circumferential	2.8	294.6	22.2
		4.2	326.9	23.3
		5.6	318.8	22.6
	Longitudinal	2.8	63.23	9.88
		4.2	56.27	8.77
		5.6	50.19	9.07
PFRP	Inner arc	3.9	263.5	22.4
	outer arc	3.7	216.4	28.1
	Rib	3.1	394.2	30.8

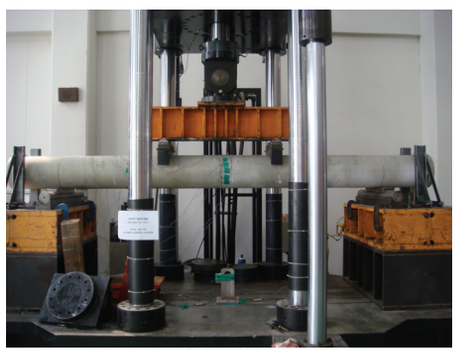

Fig. 7 Testing Set-up for Flexural Test on HCFFT Specimen (Kang, 2012)

The failure mode of specimens was that the FFRP in the tension zone was delaminated as shown in Fig. 8. The test results are summarized as given in Table 3 (Choi, et al., 2012; Kang, 2012). In Table 3, the average of test results are also summarized, respectively. In addition, the values of maximum load and moment at failure are same because specimen were tested under 4-point bending loads and the distance between support and loading point is $1m$ as shown in Fig. 6.

Fig. 8 Failure Mode of HCFFT Specimens under Flexure (Kang, 2012)

Table 3. Results of Flexural Test on the HCFFT Specimens (Kang, 2012)

Specimen No.	FFRP Thickness (t_f, mm)	Maximum Load (P, kN)		Moment at Failure (M, kNm)	
2.8-1	2.8	367	353	367	353
2.8-2		395		395	
2.8-3		297		297	
4.2-1	4.2	376	352	376	352
4.2-2		356		356	
4.2-3		323		323	
5.6-1	5.6	393	397	393	397
5.6-2		352		352	
5.6-3		447		447	

4. COMPARISON OF RESULTS

In this paper, analytical results are compared with the experimental results to estimate the accuracy of flexural analysis procedures. In the flexural analysis procedures, the cross-section of PFRP is considered separated as the inner arc, outer arc, and rib.

From the results of comparison, it is known that the results obtained by the plastic stress distribution method is different from the experimental results as much as 12.38%, 10.28%, and 18.78% when the thickness of FFRP is 2.8mm, 4.2mm, and 5.6mm, respectively. Moreover, the results obtained by the strain compatibility method is different from the experimental results as much as 37.85%, 36.14%, and 42.01% when the thickness of FFRP is 2.8mm, 4.2 mm, and 5.6mm, respectively. These comparison results are shown in Table 4. In Table 4, it can be found that the results of strain compatibility method is more conservative than the results of plastic stress distribution method. However, the results of plastic stress distribution method are more close to the experimental results than the results of strain compatibility method.

Table 4. Comparison between Experimental and Analytical Results about Flexural Strength of HCFFT

FFRP Thick-ness (t_f, mm)	Average Test Results ($M_{n(exp)}$, kNm)	Analytical Results			
		Plastic Stress Distribution Method ($M_{n(PSDM)}$)		Strain Compatibility Method ($M_{n(SCM)}$)	
		Results (kNm)	$\frac{M_{n(PSDM)}}{M_{n(exp)}}$ (%)	Results (kNm)	$\frac{M_{n(SCM)}}{M_{n(exp)}}$ (%)
2.8	353	309.30	87.62	219.39	62.15
4.2	352	315.81	89.72	224.77	63.86
5.6	397	322.46	81.22	230.24	57.99

5. CONCLUSION

In this paper, we present the analysis procedures of HCFFT piles under flexure. Two analysis procedures, i.e. the plastic stress distribution method and the strain compatibility method, are discussed. Moreover, the analytical results obtained by two analysis procedures are compared with the test results to estimate the accuracy.

The results obtained by the plastic stress distribution method are more accurate than that obtained by the strain compatibility method. The results obtained by the strain compatibility method are more conservative than that obtained by the plastic stress distribution method.

For the future study, the P-M interaction curve of HCFFT members under eccentric loading should be studied to find the axial-flexural interaction behavior.

ACKNOWLEDGEMENT

This research was supported by the Construction Technology Innovation Program (CTIP) (code: 11CCTI-C053526-03) of the Korea Institute of Construction & Technology Evaluation and Planning (KICTEP). The financial support provided by the KICTEP is acknowledged.

References

American Concrete Institute (2008a), *Building Code Requirements for Structural Concrete and Commentary (ACI 318-08)*, ACI Committee 318, Farmington Hills, Michigan.

American Concrete Institute (2008b), *Fiber-Reinforced Polymer Reinforcement for Concrete Structures (ACI 440R)*, ACI Committee 440, Farmington Hills, Michigan.

American Institute of Steel Construction (2005), *Specification for Structural Steel Building*, AISC, Inc., Chicago, Illinois.

An, D. J. (2011), Structural Characteristics of Hybrid FRP-Concrete Composite Piles, *Ph. D. Thesis*, Department of Civil Engineering, Hongik University, Seoul, Korea. (in Korean).

Beheshti-Aval, S. B. (2012), "Strength Evaluation of Concrete Filled Steel Tubes Subjected to Axial-Flexural Loading by ACI and AISC-LRFD codes along with Three Dimensional Nonlinear Analysis," *International Journal of Civil Engineering*, Vol. 10, No. 4, pp. 280-290.

Choi, J. W., Joo, H. J., Kang, I. K., and Yoon, S. J. (2012), "Design of Hybrid FRP-Concrete Composite Circular Members under Compression and Flexure," *The 2nd International Conference on Advanced Polymer Matrix Composites,* Harbin, China, pp. 22-25.

Choi, J. W., Joo, H. J., Nam, J. H., and Yoon, S. J. (2010), "Development of Hybrid CFFT Pile," *Journal of the Korean Society for Advanced Composite Structures,* Vol. 1, No. 2, pp. 20-28. (in Korean).

Choi, J. W., Lee, Y. G., Joo, H. J., Kang, I. K., and Yoon, S. J. (2011a), "Load Carrying Capacity of Hybrid FRP-Conrete Composite Compression Members," *The 2011 World Congress on Advances in Structural Engineering and Mechanics,* Vol. 18-22, pp. 4197-4205.

Choi, J. W., Park, J. S., Nam, J. H., An, D. J., and Yoon, S. J. (2011b), "An Experimental Study for the Compression Strength of Hybrid CFFT Pile," *Journal of the Korean Society for Advanced Composite Structures,* Vol. 2, No. 1, pp. 30-39. (in Korean).

Fam, A. Z. and Rizkalla, S. H. (2002), "Flexural Behavior of Concrete Filled Fiber-Reinforced polymer Circular Tube," *Journal of Composites for Construction*, Vol. 6, No. 2, pp. 123-132.

Kang, I. K. (2012), *A Study on the Development of FRP-Concrete Composite Pile*, Technical Research Report. (in Korean).

Kim, H. S. (2010). Analysis on the Flexural Behavior of Composite Bridge with CFT Girder, *MS Thesis*, Korea University, Seoul, Korea. (in Korean).

Lee, Y. G., Choi, J. W., Park, J. S., and Yoon, S. J. (2011), "Compression Strength Test of FRP Reinforced Concrete Composite Pile," *Journal of the Korean Society for Advanced Composite Structures,* Vol. 2, No. 4, pp. 19-27. (in Korean).

Shin, K. Y. (2011), Estimation of Load Carrying Capacity of Hybrid FRP-Concrete Composite Pile, *Ph. D. Thesis,* Department of Civil Engineering, Hongik University, Seoul, Korea. (in Korean).